Improving Texture Recognition using Combined GLCM and Wavelet Features

Ranjan Parekh
School of Education Technology
Jadavpur University
Kolkata, India

ABSTRACT
Texture is an important perceptual property of images based on which image content can be characterized and searched for in a Content Based Search and Retrieval (CBSR) system. This paper investigates techniques for improving texture recognition accuracy by using a set of Wavelet Decomposition Matrices (WDM) in conjunction with Grey Level Co-occurrence Matrices (GLCM). The texture image is decomposed at 3 levels using a 2D Haar Wavelet and a coefficient computed from the decomposition matrices is combined with features derived from a set of normalized symmetrical GLCMs computed along four directions, to provide improved accuracy. The proposed scheme is tested on a set of 13 textures derived from the Brodatz database and is seen to provide accuracies of the order of 90%.

General Terms
Pattern Recognition, Computer Vision, Wavelet Representation

Keywords
Texture recognition, Grey Level Co-occurrence Matrix, Wavelet decomposition, Content Based Storage and Retrieval, Pattern Recognition.

1. INTRODUCTION
In recent years the number of digital media repositories have grown exponentially, especially over the Web. Retrieving images from these repositories has, therefore, become an important research issue. With this ever expanding multimedia repository a fast and efficient search and retrieval system has become a necessity; because, without it an image repository becomes like a library of books without a catalogue - even though the information is present it is practically inaccessible to someone with specific search criteria. Texture is one of the important perceptual characteristics based on which image content can be characterized and searched. A popular texture recognition technique relates to Grey Level Co-occurrence Matrix (GLCM), proposed by Haralick (1979) and subsequently used in a number of research works. The present work investigates techniques for improving the texture recognition accuracy by using a set of Wavelet Decomposition Matrices (WDM); it also demonstrates further improvement when GLCM is used in conjunction with WDM.

The organization of the paper is as follows: section 2 provides an overview of related work, section 3 outlines the proposed approach with discussions on overview, feature computation and classification schemes, section 4 provides details of the dataset and experimental results obtained and section 5 provides the overall conclusion and the scope for future research.

2. PREVIOUS WORK
Texture refers to visual patterns or spatial arrangement of pixels that regional intensity or color alone cannot sufficiently describe. It is difficult to obtain a general mathematical model for various textures because of the large variation in their properties. A first example of the derivation of features using operators is the set of texture energy measures formulated by Laws in [1]. In [2] the authors derive texture operators from co-occurrence matrices. A simple operator for fast discrimination between textures and uniform regions has been proposed in [3]. Another method similar to Laws is described in [4]. Here a set of simple masks (vertical, horizontal, diagonal and anti-diagonal) are applied. Authors like Tamura [5] made an attempt at defining a set of visually relevant texture features. This includes coarseness, contrast, directionality, line-likeness, regularity, roughness. Fractal functions have received a great deal of attention in recent years. Pentland [6] reports a high degree of correlation between fractal dimensions and human estimates of roughness. Because of this correlation and the natural appearance of fractal generated textures, Pentland has proposed fractal functions as texture models. In [7] the authors describe a parallel algorithm for segmentation using simultaneous auto-regressive (SAR) random field models and multi-dimensional cluster analysis. In [8] the author proposes a two state Markov model to detect texture edges characterized by changes in first order statistics. Gabor filters have been used in several image analysis applications including texture classification and segmentation [9, 10]. Bovik et al [9] suggest the restriction of the choice of Gabor filters to those with isometric gaussians (aspect ratio one). In [11] the authors have used the one sided linear prediction (OSP) model, popularly known as auto-regressive (AR) model, to derive texture descriptors in terms of the prediction coefficients.

3. PROPOSED APPROACH

3.1 GLCM : An Overview
GLCM (Grey Level Co-occurrence Matrix) introduced by Haralick [12] provides one of the most popular statistical methods in analysis of grey tones in an image. The matrix defines the probability that grey level *i* occurs at a distance *d* in direction θ from grey level *j* in the texture image. These probabilities create the co-occurrence matrix $M(i, j \mid d, \theta)$. The *symmetrical* GLCM is formed by taking the transpose of the GLCM and adding it to the original GLCM. The *normalized*

symmetrical GLCM is formed by dividing each element of the GLCM with the sum of all elements. As an example, if *A* be a section of an image with corresponding data matrix then the GLCM computed along 0° (horizontal) with distance offset *d*=1 is given by *G*, and G_0 represents the normalized symmetrical version of *G*.

$$A=\begin{bmatrix}0&0&1&1\\0&0&1&1\\0&2&2&2\\2&2&3&3\end{bmatrix} \quad G=\begin{bmatrix}2&2&1&0\\0&2&0&0\\0&0&3&1\\0&0&0&1\end{bmatrix}$$

$$G_0=\frac{1}{24}\begin{bmatrix}4&2&1&0\\2&4&0&0\\1&0&6&1\\0&0&1&2\end{bmatrix}$$

Directional GLCMs might be computed along three other directions : vertical (θ = 90º and 270º), right diagonal (θ = 45º and 225º), left diagonal (θ = 135º and 315º).

$$G_{45}=\frac{1}{18}\begin{bmatrix}4&1&0&0\\1&2&2&0\\0&2&4&1\\0&0&1&0\end{bmatrix} \quad G_{90}=\frac{1}{24}\begin{bmatrix}6&0&2&0\\0&4&2&0\\2&2&2&2\\0&0&2&0\end{bmatrix}$$

$$G_{135}=\frac{1}{18}\begin{bmatrix}2&1&3&0\\1&2&1&0\\3&1&0&2\\0&0&2&0\end{bmatrix}$$

3.2 GLCM based Features

Four of the most popular features derived from a set of four directional normalized symmetrical GLCMs have been considered here viz. GLCM contrast (G_C), GLCM homogeneity (G_H), GLCM mean (G_M) and GLCM variance (G_V), as defined below. If $G_{i,j}$ represents the element (i, j) of a normalized symmetrical GLCM, and N the number of grey levels, then

$$G_C=\sum_{i=1}^{N}\sum_{j=1}^{N}G_{i,j}(i-j)^2 \tag{1}$$

$$G_H=\sum_{i=1}^{N}\sum_{j=1}^{N}\frac{G_{i,j}}{1+(i-j)^2} \tag{2}$$

$$G_M=M_i=\sum_{i=1}^{N}\sum_{j=1}^{N}iG_{i,j}=M_j=\sum_{i,j=1}^{N}\sum_{j=1}^{N}jG_{i,j} \tag{3}$$

$$G_V=\sum_{i=1}^{N}\sum_{j=1}^{N}G_{i,j}(i-M_i)^2=\sum_{i=1}^{N}\sum_{j=1}^{N}G_{i,j}(j-M_j)^2 \tag{4}$$

3.3 GLCM based Classification

A texture class consists of a set of member images : $T_i=\{t_1,t_2,...,t_n\}_i$ .For each member image, four directional GLCMs are computed :

$$T_i=\{(t^{G}{}_0,t^{G}{}_{45},t^{G}{}_{90},t^{G}{}_{135})_1,...,(t^{G}{}_0,t^{G}{}_{45},t^{G}{}_{90},t^{G}{}_{135})_n\}_i \tag{5}$$

For each member image average values of contrast, homogeneity, mean and variance are computed over the four directional GLCMs

$$T_i=[(\bar{t}^{G}{}_C,\bar{t}^{G}{}_H,\bar{t}^{G}{}_M,\bar{t}^{G}{}_V)_{1,i},...,(\bar{t}^{G}{}_C,\bar{t}^{G}{}_H,\bar{t}^{G}{}_M,\bar{t}^{G}{}_V)_{n,i}] \tag{6}$$

The texture class is then mapped with the boundary values (min / max) of its features for its member images

$$T_i=(\bar{t}^{G}{}_{X,\min},\bar{t}^{G}{}_{X,\max})_i, \quad X\in\{C,H,M,V\} \tag{7}$$

A test image s_j is assigned a weight of 1 for T_i for each of the following conditions i.e. its average GLCM feature value lies within the boundary values of the training set

$$\begin{aligned}\bar{t}^{G}{}_{C,\max,i}\geq\bar{s}^{G}{}_{C,j}\geq\bar{t}^{G}{}_{C,\min,i};\\ \bar{t}^{G}{}_{H,\max,i}\geq\bar{s}^{G}{}_{H,j}\geq\bar{t}^{G}{}_{H,\min,i};\\ \bar{t}^{G}{}_{M,\max,i}\geq\bar{s}^{G}{}_{M,j}\geq\bar{t}^{G}{}_{M,\min,i};\\ \bar{t}^{G}{}_{V,\max,i}\geq\bar{s}^{G}{}_{V,j}\geq\bar{t}^{G}{}_{V,\min,i}\end{aligned} \tag{8}$$

A cumulative weight is calculated over all the four features for all texture classes being satisfied,

$$s_j\rightarrow T_a(\omega_a),T_b(\omega_b),T_c(\omega_c),... \tag{9}$$

The test sample is assigned the class with the maximum weight, if present, otherwise a $\times$ (not determinable).

$$\begin{aligned}&s_j\rightarrow T_a,\ if\ \ \omega_a>\omega_b,\omega_c,...\\ &s_j\rightarrow\times,\ otherwise\end{aligned} \tag{10}$$

3.4 WDM : An Overview

WDM (Wavelet Decomposition Matrix) is derived from a Wavelet decomposition of the images. A *Wavelet* [13] is a mathematical function used to analyze a time dependent signal at different resolutions. The Discrete Wavelet Transform (DWT) analyses the signal at different resolutions by decomposing it into an *approximation* coefficient and a set of *detail* coefficients. The Haar Wavelet, proposed by Alfred Haar, transforms a 1-D signal into a set of averages and differences :

$$\mathbf{x}=(x_1,x_2,...,x_N)\rightarrow(s_1,...,s_{N/2}\,|\,d_1,...,d_{N/2}) \tag{11}$$

where,

$$s_k = \frac{x_{2k-1} + x_{2k}}{2}, \quad d_k = \frac{x_{2k-1} - x_{2k}}{2}, \quad k = 1, ..., N/2$$

As an example the Haar Wavelet transform for a 4-element 1-D signal is given by

$$W_4.X = \frac{1}{2}\begin{bmatrix} 1 & 1 & 0 & 0 \\ 0 & 0 & 1 & 1 \\ 1 & -1 & 0 & 0 \\ 0 & 0 & 1 & -1 \end{bmatrix}.\begin{bmatrix} x_1 \\ x_2 \\ x_3 \\ x_4 \end{bmatrix} = \frac{1}{2}\begin{bmatrix} x_1 + x_2 \\ x_3 + x_4 \\ x_1 - x_2 \\ x_3 - x_4 \end{bmatrix} \quad (12)$$

For a 2-D signal matrix *A* (N×N) the corresponding Haar Wavelet transform is defined as :

$$W_N.A.W_N^T = \begin{bmatrix} B & V \\ H & D \end{bmatrix} \quad (13)$$

where, B is the blur or approximation coefficient and H_n, V_n, D_n are the horizontal, vertical and diagonal detailed coefficients at level n. The B matrix of a specific level is used as the data matrix for the next level. The above four matrices are referred to as Wavelet Decomposition Matrices (WDM).

3.5 WDM based Features

The texture image is decomposed using a Haar Wavelet with 3-level decomposition producing following coefficients $B, H_1, V_1, D_1, H_2, V_2, D_2, H_3, V_3, D_3$, where, B is the blur or approximation coefficient and H_n, V_n, D_n are the horizontal, vertical and diagonal detailed coefficients at level n.The data matrix is partitioned into cells each 2 ×2,

$$\begin{bmatrix} a_{11} & a_{12} \\ a_{21} & a_{22} \end{bmatrix}$$

Each coefficient matrix at level 1 is computed as shown below,

$$\begin{aligned} B(i,j) &= \tfrac{1}{4}(a_{11} + a_{12} + a_{21} + a_{22}) \\ H(i,j) &= \tfrac{1}{4}\{(a_{11} + a_{12}) - (a_{21} + a_{22})\} \\ V(i,j) &= \tfrac{1}{4}\{(a_{11} + a_{21}) - (a_{12} + a_{22})\} \\ D(i,j) &= \tfrac{1}{4}\{(a_{11} + a_{22}) - (a_{12} + a_{21})\} \end{aligned} \quad (14)$$

For the second level decomposition B_1 is considered the data matrix and B_2, H_2, V_2, D_2 are similarly calculated. For the third level, B_2 is considered the data matrix and B_3, H_3, V_3, D_3 are likewise computed. B_3 is represented as B, the final blur component. A set of *covariance matrices* are computed from the detail coefficients and represented as,

$$C_{H_1}, C_{V_1}, C_{D_1}, C_{H_2}, C_{V_2}, C_{D_2}, C_{H_3}, C_{V_3}, C_{D_3}$$

For an *m* × *n* data matrix, **A** the covariance matrix is defined as,

$$C_{i,j} = C_{j,i} = \frac{1}{m-1}\sum_{k=1}^{m}\{(a_{k,i} - \mu_i)(a_{k,j} - \mu_j)\} \quad (15)$$

where, $\mu_i = \frac{a_{1,i} + a_{2,i} + ... + a_{m,i}}{m}$, m being the number of rows in A.

A set of *correlation matrices* $\Re_{H_1}, \Re_{V_1}, \Re_{D_1}, \Re_{H_2}, \Re_{V_2}, \Re_{D_2}, \Re_{H_3}, \Re_{V_3}, \Re_{D_3}$ are computed from the covariance matrices where,

$$\Re_{i,j} = \frac{C_{i,j}}{\sqrt{C_{i,i}.C_{j,j}}} \quad (16)$$

The Wavelet combined feature coefficient is computed as follows,

$$\begin{aligned} \mathbf{t}^W = \{&\mu(B), \sigma(B), \\ &\mu(\Re_{H_1}), \sigma(H_1), \mu(\Re_{V_1}), \sigma(V_1), \mu(\Re_{D_1}), \sigma(D_1), \\ &\mu(\Re_{H_2}), \sigma(H_2), \mu(\Re_{V_2}), \sigma(V_2), \mu(\Re_{D_2}), \sigma(D_2), \\ &\mu(\Re_{H_3}), \sigma(H_3), \mu(\Re_{V_3}), \sigma(V_3), \mu(\Re_{D_3}), \sigma(D_3)\} \end{aligned} \quad (17)$$

where $\mu(x_1, x_2, ..., x_n) = \frac{x_1 + x_2 + ... + x_n}{n}$ and

$\sigma(x_1, x_2, ..., x_n) = \sqrt{\frac{1}{n-1}\sum_{i=1}^{n}(x_i - \mu)^2}$.

3.6 WDM based Classification

A texture class consists of a set of member images : $T_i = \{t_1, t_2, ..., t_n\}_i$. For each member image, a Wavelet combined feature coefficient is computed

$$T_i = \{t^W{}_1, t^W{}_2, ..., t^W{}_n\}_i \quad (18)$$

The texture class is mapped to the boundary values of its feature for its member images

$$T_i = \{t^W{}_{\max}, t^W{}_{\min}\}_i \quad (19)$$

A test image s_j is assigned a weight of 3 for texture class T_i if the its Wavelet coefficient satisfies the following condition,

$$t^W{}_{\max,i} \geq s^W{}_j \geq t^W{}_{\min,i}; \quad (20)$$

The test image is then mapped to all the corresponding texture classes, if present, otherwise assigned a class ×,

$$s_j \rightarrow T_a, T_b, T_c ... \quad (21)$$

4. EXPERIMENTATIONS

Texture samples, used from the texture database of the Signal and Image Processing Institute, Electrical Engineering Department, University of Southern California, available at : http://sipi.usc.edu/database which in turn have been derived from the Brodatz texture database [14], are divided into 13 categories : bark (D12), brick wall (D94), plastic bubbles (D112), grass (D9), pressed calf leather (D24), pigskin (D92), raffia (D84), beach sand (D29), straw (D15), water (D38), herringbone weave (D16), wood grain (D68), woolen cloth (D19). Each image is 512 by 512 pixels, 8 bits/pixel grayscale mode. (Fig. 1)

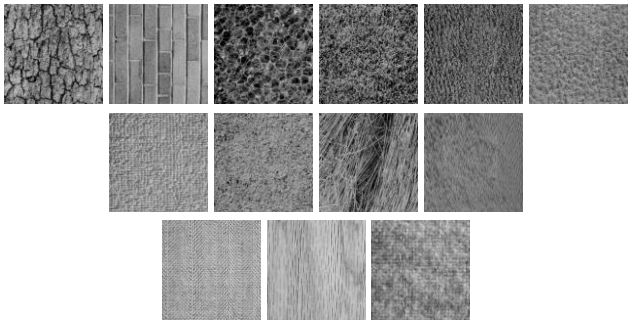

Fig 1 : Texture samples: bark, brick, bubbles, grass, leather, pigskin, raffia, sand, straw, water, weave, wood, wool

For each category four member images have been used with rotated at angles 0°, 60°, 120° and 200° angles, making a total of 52 images in the training data set. The rotated images for the "brick" texture class are shown in Fig. 2.

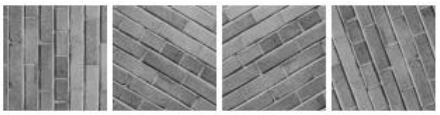

Fig 2 :Images of "brick" texture rotated at 0°, 60°, 120°, 200°

For GLCM based classification, four directional GLCMs are computed for each member image and for each GLCM four features i.e. GLCM Contrast, GLCM Homogeneity, GLCM Mean and GLCM Variance are computed, which are then averaged over the four directional GLCMs (Table 1). For WDM based classification, the WDM coefficient values are computed for each member image and the boundary values tabulated (Table 2).

Table 1. GLCM boundary values for training set

Features	GLCM Contrast		GLCM Homogeneity	
Textures	**Min**	**Max**	**Min**	**Max**
Bark	339.0615	360.4260	0.0849	0.0857
Brick	171.4014	179.7685	0.1229	0.1308
Bubbles	293.0699	324.1034	0.1145	0.1267
Grass	915.6591	1095.811	0.0723	0.1064
Leather	606.2629	688.7820	0.0576	0.0598
Pigskin	153.2743	159.1169	0.1095	0.1108
Raffia	159.8644	170.4513	0.1244	0.1305
Sand	199.5545	210.7270	0.1158	0.1175
Straw	468.5335	601.9059	0.0726	0.0823
Water	90.8227	106.4616	0.1308	0.1414
Weave	236.5369	242.4293	0.0939	0.0959
Wood	139.8697	170.6442	0.1705	0.1967
Wool	151.1335	177.1072	0.0991	0.1053
Features	**GLCM Mean**		**GLCM Variance**	
Textures	**Min**	**Max**	**Min**	**Max**
Bark	114.6904	116.3093	1921.023	2003.068
Brick	130.8294	135.8444	894.7406	971.2114
Bubbles	75.9412	83.1068	1731.717	1848.452
Grass	89.9808	97.4626	2203.103	2568.942
Leather	86.7322	90.2151	1530.442	1688.228
Pigskin	124.7919	127.1529	567.6617	583.0772
Raffia	142.9006	146.2553	665.4577	724.4272
Sand	127.5578	129.5074	707.7082	754.5747
Straw	106.0127	109.9994	1873.337	2061.593
Water	117.4929	120.4955	298.0885	322.4701
Weave	161.3729	164.0402	681.5290	697.8408
Wood	169.8766	173.9048	474.4028	530.6977
Wool	131.4930	139.0376	665.0775	718.7822

Table 2. WDM coefficient values for training set

Class	Min	Max
Bark	910.2786	923.5560
Brick	1039.1673	1080.2051
Bubbles	600.4989	657.8325
Grass	712.4310	772.4053
Leather	686.2770	714.3604
Pigskin	990.4948	1009.4092
Raffia	1135.3279	1162.2421
Sand	1012.7492	1028.3194
Straw	840.9003	873.4186
Water	932.2509	956.1594
Weave	1283.0278	1304.3172
Wood	1351.1059	1383.5352
Wool	1044.2499	1104.3967

The test data set consist of 3 images from each category but now rotated by angles of 30º, 90º and 150º, making a total of 39 images. Samples for the "brick" class are shown in Fig. 3.

Fig 3 : Images of "brick" texture rotated at 30°, 90° and 150°

The test images are numbered T1 to T39 as detailed below : T1-T3: Bark (Ba), T4-T6: Brick (Br), T7-T9: Bubbles (Bu), T10-T12: Grass (Gr), T13-T15: Leather (Le), T16-T18: Pigskin (Pi), T19-T21: Raffia (Ra), T22-T24: Sand (Sa), T25-T27: Straw (St), T28-T30: Water (Wa), T31-T33: Weave (We), T34-T36: Wood (Wd), T37-T39: Wool (Wl).

For GLCM based classification, average feature values are computed over the directional GLCMs for each test image. Based on the range of values observed during the training phase, confidence grids are constructed for classifying the test samples

into respective categories (Table 3). A test image is assigned a weight of 1 for a texture class if its average GLCM feature value lies within the boundary values of the training set for that class, otherwise denoted by a '×' (cannot be determined). The last column denotes the probable class of the test sample with the maximum weight shown in parenthesis. The samples correctly classified are shown in bold. The classification accuracy is 27 out of 39 i.e. 69.23%.

Table 3 : GLCM based Classification

#	C	H	M	V	P. Class
T1	Ba	Ba,Gr	Ba	Ba,St	**Ba** (4)
T2	Ba	Gr	Ba	St	**Ba** (2)
T3	Ba	Gr	Ba	Ba,St	**Ba** (3)
T4	Br, Wd	Br, Ra	Br,Wd	×	**Br** (3)
T5	×	Br,Bu,Ra	Br,Wd	Br	**Br** (3)
T6	Br,Wd	Br,Ra	Br,Wd	Br	**Br** (4)
T7	×	×	×	Le	Le (1)
T8	Ba	×	×	Ba,St	Ba (2)
T9	Bu	×	Bu	×	**Bu** (2)
T10	Gr	Gr,Wd	Gr	Gr	**Gr** (4)
T11	×	×	×	×	×
T12	×	Gr,St	Gr	×	**Gr** (2)
T13	Le	Le	Le	Le	**Le** (4)
T14	×	Le	Le	X	**Le** (2)
T15	Le	Le	Le	Le	**Le** (4)
T16	Ra,Wd,Wl	×	×	×	×
T17	Wd,Wl	×	Pi	×	×
T18	Ra,Wd,Wl	×	Pi	×	×
T19	Wd,Wl	Br,Ra	×	×	×
T20	Pi,Wd,Wl	Wa	Ra	Ra,We,Wl	×
T21	Wl	Br,Bu	Ra	Sa	×
T22	Sa	Bu,Sa	Sa	Sa	**Sa** (4)
T23	×	Bu	Sa	×	×
T24	×	Bu	Pi	Sa	×
T25	St	Gr,St	St	Ba,St	**St** (4)
T26	St	Gr,St	×	St	**St** (3)
T27	St	Gr,St	St	Ba,St	**St** (4)
T28	Wa	Wa	×	Wa	**Wa** (3)
T29	×	Wa	Wa	Wa	**Wa** (3)
T30	Wa	Wa	×	Wa	**Wa** (3)
T31	×	Gr,We	X	Ra,Wl	×
T32	×	Gr,We	We	Ra,We,Wl	**We** (3)
T33	We	Gr,We	We	Ra,We,Wl	**We** (3)
T34	Wd	Wd	Wd	Wd	**Wd** (4)
T35	Br,Wl	Wd	Wd	Wd	**Wd** (3)
T36	Pi,Wd,Wl	Wd	Wd	Wd	**Wd** (4)
T37	Pi,Wd,Wl	Gr,Wl	Wl	Ra,Wl	**Wl** (4)
T38	Br,Wl	Gr,Wl	Wl	Ra,We,Wl	**Wl** (4)
T39	Ra,Wd,Wl	Gr,Wl	Br,Wl	Ra,Wl	**Wl** (4)

For WDM based classification, Wavelet coefficient values are computed for each test image. A test image is assigned a weight of 3 for a texture class if its Wavelet coefficient value lies within the boundary values of the training set for that class, otherwise denoted by a '×' (Table 4). 34 out of 39 test samples are correctly classified (indicated by bold), providing an accuracy of 87.17%

Table 4 : WDM based Classification

#	P. Class	#	P. Class	#	P. Class
T1	**Ba** (3)	T14	**Le** (3)	T27	**St** (3)
T2	**Ba** (3)	T15	**Le** (3)	T28	**Wa** (3)
T3	**Ba** (3)	T16	**Pi** (3)	T29	**Wa** (3)
T4	**Br** (3)	T17	**Pi** (3)	T30	**Wa** (3)
T5	**Br** (3)	T18	**Pi** (3)	T31	**We** (3)
T6	**Br** (3)	T19	**Ra** (3)	T32	**We** (3)
T7	Le (3)	T20	**Ra** (3)	T33	**We** (3)
T8	**Bu** (3)	T21	**Ra** (3)	T34	**Wd** (3)
T9	**Bu** (3)	T22	**Sa** (3)	T35	**Wd** (3)
T10	Le (3)	T23	**Sa** (3)	T36	**Wd** (3)
T11	**Gr** (3)	T24	Pi (3)	T37	**Wl** (3)
T12	**Gr** (3)	T25	**St** (3)	T38	Br (3)
T13	**Le** (3)	T26	**St** (3)	T39	Br (3)

For a combined GLCM + WDM classification, a sample is assigned a texture class with a higher weightage, if the class estimate based on the GLCM and WDM classifications are different, or assigned a class '×' if weights for different classes are equal.

$$\left.\begin{matrix} s_j \overset{GLCM}{\rightarrow} T_a(\omega_a) \\ s_j \overset{DWT}{\rightarrow} T_b(\omega_b) \end{matrix}\right\} \begin{matrix} s_j \rightarrow T_a,\ if\ T_a \neq T_b\ \&\ \omega_a > \omega_b \\ s_j \rightarrow T_b,\ if\ T_a \neq T_b\ \&\ \omega_b > \omega_a \end{matrix} \quad (22)$$

The "C" column denotes the probable class of the test sample taking into account both the GLCM (G) and WDM (W) classifications and assigning the texture class with the higher weight to the test sample. The samples correctly classified are indicated in bold. The classification accuracy is 37 out of 39 i.e. 94.87%

Table 5 : Combined Classification

#	G	W	C	#	G	W	C
T1	Ba (4)	Ba (3)	**Ba**	T21	×	Ra (3)	**Ra**
T2	Ba (2)	Ba (3)	**Ba**	T22	Sa (4)	Sa (3)	**Sa**
T3	Ba (3)	Ba (3)	**Ba**	T23	×	Sa (3)	**Sa**
T4	Br (3)	Br (3)	**Br**	T24	×	Pi (3)	Pi
T5	Br (3)	Br (3)	**Br**	T25	St (4)	St (3)	**St**
T6	Br (4)	Br (3)	**Br**	T26	St (3)	St (3)	**St**
T7	Le (1)	Le (3)	Le	T27	St (4)	St (3)	**St**
T8	Ba (2)	Bu (3)	**Bu**	T28	Wa (3)	Wa (3)	**Wa**
T9	Bu (2)	Bu (3)	**Bu**	T29	Wa (3)	Wa (3)	**Wa**
T10	Gr (4)	Le (3)	**Gr**	T30	Wa (3)	Wa (3)	**Wa**
T11	×	Gr (3)	**Gr**	T31	×	We (3)	**We**
T12	Gr (2)	Gr (3)	**Gr**	T32	We (3)	We (3)	**We**
T13	Le (4)	Le (3)	**Le**	T33	We (3)	We (3)	**We**
T14	Le (2)	Le (3)	**Le**	T34	Wd (4)	Wd(3)	**Wd**
T15	Le (4)	Le (3)	**Le**	T35	Wd (3)	Wd(3)	**Wd**
T16	×	Pi (3)	**Pi**	T36	Wd (4)	Wd(3)	**Wd**
T17	×	Pi (3)	**Pi**	T37	Wl (4)	Wl (3)	**Wl**
T18	×	Pi (3)	**Pi**	T38	Wl (4)	Br (3)	**Wl**
T19	×	Ra (3)	**Ra**	T39	Wl (4)	Br (3)	**Wl**
T20	×	Ra (3)	**Ra**				

5. CONCLUSIONS

This paper outlines a scheme for image texture recognition based on a three level decomposition using Haar Wavelets. Firstly the scheme has been shown to be robust to rotational variation of texture images. Secondly, it demonstrates an improvement in recognition accuracy over another popular scheme using Grey Level Co-occurrence Matrix (GLCM). Further, it has been shown that the recognition accuracy can be further improved by combining GLCMs with Wavelet Decomposition Matrices. However, additional measures are required to address the problems related to variations in brightness, contrast and tonal range of the images. One way to tackle this problem is via histogram normalization; another methodology providing scope for further research is to combine color and texture, e.g. wood textures combined with its various hues.

6. REFERENCES

[1] Laws, K. I. 1980. Textured image segmentation. Doctoral Thesis. University of Southern California, Los Angeles, CA, USCIPI Rep. 940.

[2] Conners, R. W., Trivedi, M. M., and Harlow, C. A. 1984. Segmentation of a High Resolution Urban Scene using Texture Operators. Computer Vision, Graphics and Image Processing, vol. 25, 273-310.

[3] Dinstein, I., Fong, A. C., Ni, L. M., and Wong, K. Y. 1984. Fast Discrimination between Homogeneous and Textured Regions. In Proceedings of the 7th International Conference on Pattern Recognition, Montreal, Canada, 361-363.

[4] Wang, R., Hanson, A. R. and Riseman, E. M. 1986. Texture Analysis based on Local Standard Deviation of Intensity. In Proceedings of the Conference on Computer Vision and Pattern Recognition, Florida, USA, 481-488.

[5] Tamura, H., Mori, S., and Yamawaki, T. 1978. Textural Features corresponding to Visual Perceptions. IEEE Transactions on Systems, Man and Cybernetics, vol. 8, no. 6, 460-473.

[6] Pentland, A. P. 1984. Fractal based Description of Natural Scenes. IEEE Transactions on Pattern Analysis and Machine Intelligence, vol. 6, no. 6, 661-674.

[7] Khotanzad, A., and Bouarfa, A. 1988. A Parallel Non-parametric Non-iterative Clustering Algorithm with Application to Image Segmentation. In Proceedings of the 22nd Asilomar Conference on Signals, Systems and Computers, Pacific Grove, CA, 305-309.

[8] Huang, N. K. 1984. Markov Model for Image Segmentation. In Proceedings of the 22nd Allerton Conference on Communication, Control and Computing, Montecello, 775-781.

[9] Bovik, A. C., Clark, M., and Geisler, W. S. 1990. Multichannel Texture Analysis using Localized Spatial Filters. IEEE Transactions on Pattern Analysis and Machine Intelligence, vol. 12, no. 1, 55-73.

[10] Manjunath, B. S., and Chellappa, R. 1993. A Unified Approach to Boundary Perception : Edges, Textures and Illusory Contours. IEEE Transactions on Neural Networks, vol. 4, no. 1, 96-108.

[11] Deguchi, K., and Morishita, I. 1978. Texture Characterization and Texture-based Image Partitioning using Two-dimensional Linear Estimation Techniques. IEEE Transactions on Computers, vol. C-27, no. 8, 739-745.

[12] Haralick, R. M. 1979. Statistical and Structural Approaches to Texture. Proceedings of IEEE, vol. 67, 786–804.

[13] Graps, A. 1995. An Introduction to Wavelets. IEEE Computational Science and Engineering, vol. 2, no. 2, 50-61.

[14] Brodatz, P. 1966. Textures : A photographic album for artists and designers. Dover Publications, NY. (http://www.ux.uis.no/~tranden/brodatz.html)